Integrated high-resolution dataset of high intensity European and- Mediterranean flash floods

William Amponsah[1,2*], Pierre-Alain Ayral[3,4], Brice Boudevillain[5], Christophe Bouvier[6], Isabelle Braud[7], Pascal Brunet[6], Guy Delrieu[5], Jean-François Didon-Lescot[3], Eric Gaume[8], Laurent Lebouc[8], Lorenzo Marchi[9], Francesco Marra[10], Efrat Morin[10], Guillaume Nord[5], Olivier Payrastre[8], Davide Zoccatelli[10], Marco Borga[1]

[1] Department of Land, Environment, Agriculture and Forestry, University of Padova, Legnaro, Italy

[2] Department of Agricultural and Biosystems Engineering, College of Engineering, KNUST, Kumasi, Ghana

[3] ESPACE, UMR7300 CNRS, "Antenne Cevenole", Université de Nice-Sophia-Antipolis, France

[4] LGEI, IMT Mines Ales, Univ Montpellier, Ales, France

[5] Univ. Grenoble Alpes, CNRS, IRD, Grenoble INP, IGE, F-38000 Grenoble, France

[6] Hydrosciences, UMR5569 CNRS, IRD, Univ. Montpellier, Montpellier, France

[7] Irstea, UR RiverLy, Lyon-Villeurbanne Center, 68626 Villeurbanne, France

[8] IFSTTAR, GERS, EE, F-44344 Bouguenais, France

[9] CNR IRPI, Padova, Italy

[10] Institute of Earth Sciences, Hebrew University of Jerusalem, Israel

*Corresponding author: William Amponsah
Department of Agricultural and Biosystems Engineering, College of Engineering, KNUST, Kumasi, Ghana
e-mail address: wamponsah@knust.edu.gh
willzamponsah@gmail.com

Marked-up manuscript version

Abstract

This paper describes an integrated, high-resolution dataset of hydro-meteorological variables (rainfall and discharge) concerning a number of high-intensity flash floods that occurred in Europe and in the Mediterranean region from 1991 to 2015. This type of dataset is rare in the scientific literature because flash floods are typically poorly observed hydrological extremes. Valuable features of the dataset (hereinafter referred to as EuroMedeFF database) include i) its coverage of varied hydro-climatic regions, ranging from Continental Europe through the Mediterranean to Arid climates, ii) the high space-time resolution radar-rainfall estimates, and iii) the dense spatial sampling of the flood response, by observed hydrographs and/or flood peak estimates from post-flood surveys. Flash floods included in the database are selected based on the limited upstream catchment areas (up to 3000 km^2), the limited storm durations (up to 2 days), and the unit peak flood magnitude. The EuroMedeFF database comprises 49 events that occurred in France, Israel, Italy, Romania, Germany~~,~~ and Slovenia, and constitutes a sample of rainfall and flood discharge extremes in different climates. The dataset may be of help to hydrologists as well as other scientific communities because it offers benchmark data for the identification and analysis of the hydro-meteorological causative processes, evaluation of flash flood hydrological models and for hydro-meteorological forecast systems. The dataset also provides a template for the analysis of the space-time variability of flash flood-triggered rainfall fields and of the effects of their estimation on the flood response modelling. The dataset is made available to the public ~~as a "public dataset"~~ with the following DOI: https://doi.org/10.6096/MISTRALS-HyMeX.1493.

Keywords: *flash flood, radar-rainfall estimation, peak discharge estimation, prediction in ungauged basins, flood risk management*

1. Introduction

Flash floods are triggered by high-intensity and relatively short duration (up to 1-2 days) rainfall often of spatially confined convective origin (Gaume et al., 2009; Smith and Smith, 2015; Saharia et al., 2017). Due to the relatively small temporal scales, catchment scales impacted by flash floods are generally less than 2000-3000 km^2 in size (Marchi et al., 2010; Braud et al., 2016). Given the large rainfall rates and the rapid concentration of streamflow promoted by the topographic relief, flash floods often shape the upper tail of the flood frequency distribution of small to medium size catchments. Understanding the hydro-meteorological processes that control flash flooding is therefore important from both scientific and societal perspectives. On one side, elucidating flash flood processes may reveal aspects of flood response that either were unexpected on the basis of less intense rainfall input, or highlight anticipated but previously undocumented characteristics. On the other side, improved understanding of flash floods is required to better forecast these events and manage the relevant risks (Hardy et al, 2016), because knowledge based on the analysis of moderate floods may be questioned when used for forecasting the response to local extreme storms (Collier, 2007; Yatheendradas et al., 2008).

However, the relatively reduced small spatial and temporal scales of flash floods, relative to the sampling characteristics of typical hydro-meteorological networks, make these events particularly difficult to monitor and document. In most of the cases, the spatial scales of the events are generally much smaller than the sampling potential offered by even supposedly dense raingauge networks (Borga et al., 2008; Amponsah et al., 2016). Similar considerations apply to streamflow monitoring: often the flood responses are simply ungauged. In the few cases where a stream gauge is in place, streamflow monitoring is affected by major limitations. For instance, peak water levels may exceed the range of available direct discharge measurements in rating curves, causing major uncertainties in the conversion of flood stage data to discharge data. In other cases, stream gauges are damaged or even wiped out by the flood current: in these cases, only part of the hydrograph (usually a segment of the rising limb) is recorded.

The call for better observations of flash flood response has stimulated the development of a focused monitoring methodology in the last fifteen years over Europe and the Mediterranean region (Gaume et al, 2004; Marchi et al., 2009; Bouilloud et al., 2009; Calianno et al., 2013; Amponsah et al, 2016). This methodology is built on the use of post-flood surveys, where observations of traces left by water and sediments during a flood are combined with accurate topographic river sections survey to provide spatially detailed estimates of peak discharges along the stream network. However, the important thing to note here is that the survey needs to capture not only the maxima of peak discharges: less intense responses within the flood-impacted region are important as well. These can be contrasted with the corresponding generating rainfall intensities and depths obtained by weather radar re-analysis, thus permitting identification of the catchment properties controlling the rate-limiting processes (Zanon et al., 2010). The large uncertainty affecting indirect peak discharge estimates may be constrained and reduced by comparison with peak discharges obtained from hydrological models fed with rainfall estimates from weather radar and rain gauge data (Amponsah et al., 2016). Post-flood surveys typically start immediately after the event and are carried out in the following weeks and months (Gaume and Borga, 2008), during the so-called Intensive Post-Event Campaigns (IPEC, in the following), before possible obliteration of field evidence from restoration works or subsequent floods.

The aim of this paper is to outline the development of the EuroMedeFF dataset, which organises flash flood hydro-meteorological and geographical data from 49 high-intensity flash floods, whose location stretches from the western and central Mediterranean, through the Alps into Continental Europe. The database includes high-resolution radar rainfall estimates, flood hydrographs and/or flood peak estimates through IPEC, and digital terrain models (DTM) of the concerned catchments. Collation of the EuroMedeFF dataset is a challenging task (Borga et al., 2014), due (i) to the lack of conventional hydro-meteorological data which characterizes these events (owing to the small spatio-temporal scales at which these events occur), and (ii) to the fact that extreme events are, by definition, rare. Collecting rainfall and flood data by means of opportunistic post flood surveys required the mobilization of a group of researchers (ranging in size from 5 to more than 20 persons) for an extended period of time (ranging from a few days to some weeks). In addition to this, high quality weather radar estimates of extreme events such as the ones triggering flash floods are not easy to be gathered, due to the number of sources of error affecting radar estimation under heavy precipitation and in rough topography environment (Germann et al., 2006; Villarini and Krajevski, 2010). Owing to these reasons, the EuroMedeFF dataset of 49 flash flood events comprising high quality radar rainfall estimates, flood hydrographs, surveyed flood peaks at ungauged sites, and digital terrain models is simply unprecedented in size in Europe and in the Mediterranean in terms of (i) number of events, (ii) variety of provided data, and (iii) the degree of integration. ~~The archive provides high-resolution data enabling the analysis of rainfall space-time structure and flood response and the application of hydrological~~

~~models for the simulation of the flash flood response across varying hydro-climatological contexts.~~ Given the quality and resolution of the rainfall input, the archive provides unprecedented data to examine the impact of space-time resolution in the modelling of high intensity flash floods under different climate and environmental controls. Since results from previous modelling studies are quite mixed, being much of the knowledge either site-specific or expressed qualitatively, the availability of the EuroMedeFF data archive may open new avenues to synthesize this knowledge and transfer it to new situations.

~~This article is organized as follows: the~~ The criteria for the EuroMedeFF database development and a summary table and spatial locations of the collected flash floods are presented in Section 2. Section 3 describes the components of the flash flood datasets, whereas ~~The~~ the methods used to generate the rainfall and discharge datasets are presented in Section ~~3~~4. ~~Section 4 describes the components of the flash flood datasets, whereas~~ Section 5 discusses the main features of the dataset, based on climatic regions and the two methodologies for discharge data collection (stream gauges and indirect estimates from post-flood analysis). General remarks on the scientific importance of the EuroMedeFF database are provided in the Conclusions section, whereas a link to the freely accessible EuroMedeFF database is provided in the Data Availability section.

2. Criteria for EuroMedeFF database development

The EuroMedeFF database includes data from high intensity flash flood events from different hydro-climatic regions in the Euro-Mediterranean area. To be included in the data set, the following data availability were ensured: i) digital terrain model (DTM) of resolutions 5 – 90 m of the impacted region/catchment; ii) weather radar rainfall estimation with high spatial and temporal resolutions, and iii) discharge data from stream gauges and/or post-flood analyses. Rainfall data are provided at a time resolution of 60 min or less and as 'best available rainfall products' (i.e., estimates which include the merging of radar and raingauge estimates).

Three criteria have been considered for the development of the EuroMedeFF database:

i) *Flood magnitude:* A unit peak discharge of 0.5 $m^3 s^{-1} km^{-2}$ (this parameter is termed $F_{th\cancel{reshold}}$) is considered as the lowest value for defining a flash flood event. This means that, for an event to be included in the database, at least one measured flood peak should exceed the value of $F_{th\cancel{reshold}}$. The authors are aware that, depending on climate and catchment size, unit peak discharge of 0.5 $m^3 s^{-1} km^{-2}$ can correspond to a severe flash flood (for instance, in the inner sector of the alpine range) or a moderate flash flood (for instance, in many Mediterranean basins). A value of 0.5 $m^3 s^{-1} km^{-2}$ can be considered as a lower threshold for flash floods across a variety of climates and studies (Gaume et al., 2009; Marchi et al., 2010; Tarolli et al., 2012; Braud et al., 2014). For the sake of simplicity, we adopted the same value of $F_{th\cancel{reshold}}$ in all the studied regions. Since the identification of the flash floods included in the database ~~mostly derives from~~ is primarily driven by the local observed impact, for most floods the lowest unit peak discharge is much higher than $F_{th\cancel{reshold}}$.

ii) *Spatial extent:* The upper limit for a catchment impacted by the flood is 3000 km^2 (this parameter is termed $A_{th\cancel{reshold}}$). The same meteorological event may have triggered multiple floods (e.g., September and October 2014 floods in France which have affected several mesoscale catchments of about 2000 km^2 - Ardèche, Cèze, Gard and Hérault). In this case, we report several events for the same date, corresponding to different specific catchments with areas less than $A_{th\cancel{reshold}}$.

iii) *Storm duration:* The upper limit for the duration of the flood-triggering storm is up to 48 hours (this parameter is termed $D_{th\cancel{reshold}}$). The rainfall duration is identified by defining a minimum period duration with basin-averaged hourly rainfall intensity less than 1 mm/h over the impacted catchment to separate the time series in consistent events. The methodology is similar to Marchi et al. (2010) and Tarolli et al. (2012), where the duration is defined as 'the time duration of the flood-generating rainfall episodes which are separated by less than 6 h of rainfall hiatus'. We made this threshold explicit to reduce subjectivity. Here, the minimum duration depends subjectively on hydro-climatic settings and basin size. The reported $D_{th\cancel{reshold}}$ is the duration of the rainfall responsible for each event flood peak, separated from other rainfall events that may have occurred before or after the main event depending on the characteristics of the largest involved catchment. In a number of cases in which the features of the flash flood response were specifically affected by wet initial soil moisture conditions, rainfall data is provided for a longer period than the storm duration. This enables us to account for antecedent rainfall in the analyses.

In general, the preliminary selection of flash floods was based on rainfall data (amount, intensity) from meteorological agencies and qualitative field recognition of flood response. This led to exclude a number of low-intensity events. Post-flood reconstruction of peak discharge was carried out for events that passed this preliminary screening. Several of these events were not included in the dataset because they failed to meet the requirements in terms of flood magnitude, spatial extent and storm duration. Given these constraints, the EuroMedeFF database includes 49 high-intensity flash floods: 30 events in France, seven events each in Israel and in Italy, three events in Romania, one event each in Germany and in Slovenia.

Figure 1 shows the location of the basins impacted by the flash floods included in the data archive and provides information on the basic features, such as timing of occurrence over the year, size of the largest affected river basin and highest unit peak discharge. The figure shows that the timing of the floods varies gradually from the south-west, where the floods occur mainly in the September to November season, to the east, where the floods occur mainly in the period from autumn to late spring. The shift in seasonality is paralleled by a decreasing basin size and unit peak discharge from south-west to east. These findings are supported by the work of Parajka et al. (2010), who analysed the differences in the long-term regimes of extreme precipitation and floods across the Alpine-Carpathian range, and of Dayan et al. (2015) who analysed the seasonality signal of atmospheric deep convection in the Mediterranean area.

Table 1 reports summary information of the EuroMedeFF database. In the table, each event is labelled as an '*EventID*', which comprises the impacted catchment/region and the year of occurrence, e.g., ORBIEL1999 (cf. event 1 in Table 1). The '*EventID*' is used in the archive to uniquely identify ~~unequivocally~~ the event. The table is ordered first on country basis, followed by the date of flood peak for each country, from past to the most recent events. For each of the 49 events, the table reports the river basin and the country, the date of the flood peak, the climatic region, the number of river sections for which discharge data are available (both in terms of indirect post-flood estimates and streamgauge-based data), with indications of the sections with streamgauge information, the range of basin area for the catchments closed at the studied river sections, the storm duration, the range of unit peak discharges and the indication of earlier works on the event. In a few cases, more than one flash flood event is reported for the same river basin.

We used the Budyko diagram (Budyko, 1974) to characterise the climatic context of the catchments included in the EuroMedeFF database (Figure 2). The Budyko framework plots the evaporation index (i.e., the ratio of mean annual actual evaporation to mean annual precipitation, AET/P) versus the aridity index (i.e., the ratio of mean annual potential evapotranspiration to mean annual precipitation

PET/P). The mean values of these variables were calculated for each river basin, so the number of points plotted in Figure 2 is smaller than the total number of flash floods in the database. Figure 2 also reports the empirical Budyko curve (continuous curve; Budyko,1974), which fits well with the upper envelope (dotted curve) of the data included in the data archive. Not surprisingly, the catchments under Arid or Arid-Mediterranean climate display typically water-limited conditions, with the aridity index, PET/P > 1. Continental, Alpine and Alpine-Mediterranean catchments lie in the energy-limited sector of the Budyko plot, with aridity index, PET/P < 1, indicating wet climate. Mediterranean catchments often display water-limited conditions, although less severe than catchments under Arid and Arid-Mediterranean climate.

3 The EuroMedeFF dataset

The EuroMedeFF dataset consists of high-resolution data on rainfall, discharge, and topography. The information in the data archive is categorised into three main groups: *generic, spatial* and *discharge* data.

3.1 Generic data

The '*Readme'* text file contains generic data on the date of the flash flood occurrence, the name of the impacted catchment and the Country and Administrative Region of the catchment. Detailed generic information on the spatial data (DTM and radar) and discharge data (flood hydrographs and IPECs) are also elaborated in the ~~'*Readme'* text~~ file. ~~T~~Also the coordinate systems and grid sizes of the spatial data, and the time resolutions and reference of the radar and flood hydrographs are summarised. ~~in the '*Readme'* text file.~~

3.2 Spatial data

i) Topographic data: Digital Terrain Model (DTM) with a grid size of 5 - 90 m. ~~or less but coarse enough to avoid data storage problems. For this reason, we avoided providing DTM data at less than 5 m grid size.~~ For each event, DTM data are provided in compressed ASCII raster files, with label '*EventID_DTMXX*', where *XX* is the grid size in meters. DTM is provided in the local country coordinate system, with a file (*DTMXX_WGS84_LowLeft_corner*) reporting the coordinates of the low-left corner in the WGS84 coordinate system. All the data relative to one country are in the same coordinate system.

ii) *Radar-rainfall data:* Corrected and raingauge-adjusted radar-rainfall data are provided with a 1-km or less grid size and temporal resolution appropriate for the flood (typically 60 min or less). For each event, radar data are provided in compressed ASCII raster files, with label '*EventID _RADAR*'. Radar data are provided, consistent with the DTM data, in the local country coordinate system with a file (*Radar_WGS84_LowLeft_corner*) reporting the coordinates of the low-left corner in the WGS84 coordinate system. At least, all the data relative to one country are in the same coordinate system. The time reference for the radar data is provided as yymmddH_bM_b – yymmddH_eM_e with H_b, M_b referring to the beginning and H_e, M_e to the end of the considered time period.~~'*yymmddHHMM*'~~.

The spatial data (DTM and radar) are provided in ASCII format. The coordinates for radar and DTM data as well as locations of streamgauge and IPEC sections are consistently provided in both local (country-specific) and WGS84 systems. The main advantage of WGS84 is that it avoids possible conversion problems from local coordinate systems, while providing a homogeneous coordinate system throughout the database.

3.3 Discharge data

i) *Flood hydrographs:* For each event, the location of the available streamgauge stations, upstream area of the basin draining to the station and observed hydrographs are provided in the excel file '*EventID_HYDROGRAPHS*'. The coordinates are consistent with the local country coordinate system given for the spatial data, and are also provided in the WGS84 coordinate system. The time reference system for the hydrograph data are consistent with that used for the radar data.

ii) *Post-flood data:* Comprehensive data on post-flood surveys through IPEC are provided in the excel file '*EventID_IPEC*'. For each section, the location of the surveyed cross-section~~(outlet)~~, the area of the basin, the indirect estimation method used and peak discharge estimates are provided. When possible, the following further parameters are reported: flood peak time, wet area, slope, roughness parameter, mean flow velocity, Froude number, geomorphic impacts (in three classes – Marchi et al., 2016), and the estimated peak discharge uncertainty range (Amponsah et al., 2016). Coordinates of the surveyed sections are consistent with the local country coordinate system given for the spatial data, and are also provided in the WGS84 coordinate system.

~~The spatial data (DTM and radar) are provided in ASCII format, compressed to save disk space. The coordinates for radar and DTM data as well as locations of streamgauge and IPEC sections are consistently provided in both local (country-specific) and WGS84 systems. The main advantage of WGS84 is that it avoids possible conversion problems from local coordinate systems, while providing a homogeneous coordinate system throughout the database.~~

4. Rainfall and discharge estimation methods

4.1 Rainfall estimation methods

Raw radar data were provided by several sources and elaborated following different procedures depending on the quality and type of available radar and raingauge data, in order to obtain the best spatially distributed precipitation estimate for each event. In general, original reflectivity data in polar coordinates have been used as raw radar data. A set of correction procedures, taking into account the highly non-linear physics of radar detection of precipitation, and procedures for the rain gauge-based adjustment, were used. The procedures include the correction of errors due to antenna pointing, ground echoes, partial beam blockage, beam attenuation in heavy rain, vertical profile of reflectivity and wet radome attenuation, and a two-step bias adjustment that considers the range-dependent bias at yearly scale and the mean field bias at the single event scale. Radar and rain gauge rainfall estimates were merged using the same procedure: a mean field bias calculated at the event accumulation scale using rain gauges located in or around the study catchment. Additional details on the procedures can be found in Bouilloud et al. (2010), Delrieu et al. (2014), Marra et al. (2014), Marra and Morin (2015), Boudevillain et al. (2016) and in the references therein.

For French events 7, 26 and 30 in Table 1, only rainfall data from one local rain gauge is available. These floods have been kept in the database because of the interest in including flood response data for very small basins (< 1km^2) and because the small catchment size of the Valescure basin (4 km^2) causes the absence of radar rainfall data to be less detrimental than for floods that hit larger catchments. Note that the available raingauge is located within the considered 4 km^2 basin. In addition, as the radar closest was quite far from the catchment, located in a zone with complex topography, radar data accuracy was not granted.

~~3.1~~4.2 Discharge estimation methods

Discharge data in the EuroMedeFF database derive from both streamflow monitoring stations and post-flood indirect estimates of flow peak through IPEC. Streamflow data, permitting to record flood hydrographs, thus enabling to assess not only discharge but also time response and flood runoff volume estimation, were checked for the uncertainties affecting rating curves at high flood stages by using hydraulic models and topographic data. ~~monitoring permits to record flood hydrographs, thus enabling to assess not only discharge but also time response and flood runoff volume~~. Discharge data from reservoir operations, water levels and use of the continuity equation, when available, were also included into the database after accurate quality control. ~~share these valuable features with data from stream gauges~~.

Different methods have been used for the indirect reconstruction of flow velocity and peak discharge from flood marks, such as slope-area, slope-conveyance, flow-through-culvert, and lateral super-elevation in bends. Amongst these methods, the most commonly used for the implementation of the dataset presented in this paper is the slope-conveyance, which consists of the application of the Manning-Strickler equation, under assumption of uniform flow, and requires the topographic survey of cross-section geometry and flow energy gradient, computed from the elevation difference between the high water marks along the channel reach surveyed (Gaume and Borga, 2008; Lumbroso and Gaume, 2012).

Although the identification of river cross-sections suitable for indirect peak discharge assessment has sometimes proved not easy (flood marks can be hardly visible or obliterated by post-flood restoration works), ~~whereas~~ and discharge reconstruction in cross sections that underwent major topographic changes is affected by major uncertainties (Amponsah et al., 2016), an ~~wise~~ appropriate choice of the cross sections permitted to achieve a spatially-distributed representation of flood response for most studied events. Specific details on the IPEC procedures can be found in the references provided in Table 1.

~~**43 The EuroMedeFF dataset**~~

~~The EuroMedeFF dataset consists of high-resolution data on rainfall, discharge, and topography. The information in the data archive is categorised into three main groups: *generic, spatial* and *discharge* data.~~

~~4.13.1 Generic data~~

~~The '*Readme'* text file contains generic data on the date of the flash flood occurrence, the name of the impacted catchment and the Country and Administrative Region of the catchment. Detailed generic information on the spatial data (DTM and radar) and discharge data (flood hydrographs and IPECs) are also elaborated in the '*Readme'* text file. The coordinate systems and grid sizes of the spatial data, and the time resolutions and reference of the radar and flood hydrographs are summarised in the '*Readme'* text file.~~

~~4.23.1 Spatial data~~

- ~~*i) Topographic data:* Digital Terrain Model (DTM) with a grid size of 90 m or less but coarse enough to avoid data storage problems. For this reason, we avoided providing DTM data at less than 5 m grid size. For each event, DTM data are provided in compressed ASCII raster files, with label '*EventID_DTMXX*', where *XX* is the grid size in meters. DTM is provided in the local country coordinate system, with a file (*DTMXX_WGS84_LowLeft_corner*) reporting the coordinates of the low-left corner in the WGS84 coordinate system. All the data relative to one country are in the same coordinate system.~~
- ~~*ii)i)Radar-rainfall data:* Corrected and raingauge-adjusted radar-rainfall data are provided with a 1-km or less grid size and temporal resolution appropriate for the flood (typically 60 min or less). For each event, radar data are provided in compressed ASCII raster files, with label '*EventID _RADAR*'. Radar data are provided, consistent with the DTM data, in the local country coordinate system with a file (*Radar_WGS84_LowLeft_corner*) reporting the coordinates of the low-left corner in the WGS84 coordinate system. At least, all the data relative to one country are in the same coordinate system. The time reference for the radar data is provided as '*yymmddHHMM*'.~~

~~4.33.1 Discharge data~~

~~*i) Flood hydrographs:* For each event, the location of the available streamgauge stations, upstream area of the basin draining to the station and observed hydrographs are provided in the excel file '*EventID_HYDROGRAPHS*'. The coordinates are consistent with the local country coordinate system given for the spatial data, and are also provided in the WGS84 coordinate system. The time reference system for the hydrograph data are consistent with that used for the radar data.~~

~~*ii)*~~*i)*~~*Post-flood data:* Comprehensive data on post-flood surveys through IPEC are provided in the excel file '*EventID_IPEC*'. For each section, the location of the surveyed cross-section (outlet), the area of the basin, the indirect estimation method used and peak discharge estimates are provided. When possible, the following further parameters are reported: flood peak time, wet area, slope, roughness parameter, mean flow velocity, Froude number, geomorphic impacts (in three classes – Marchi et al., 2016), and the estimated peak discharge uncertainty range (Amponsah et al., 2016). Coordinates of the surveyed sections are consistent with the local country coordinate system given for the spatial data, and are also provided in the WGS84 coordinate system.~~

~~The spatial data (DTM and radar) are provided in ASCII format, compressed to save disk space. The coordinates for radar and DTM data as well as locations of streamgauge and IPEC sections are consistently provided in both local (country-specific) and WGS84 systems. The main advantage of WGS84 is that it avoids possible conversion problems from local coordinate systems, while providing a homogeneous coordinate system throughout the database.~~

5 Discussion

~~Figure 1 shows the location of the basins impacted by the flash floods included in the data archive and provides information on the basic features, such as timing of occurrence, size of the largest affected river basin and highest unit peak discharge. The figure shows that the timing of the floods varies gradually from the south-west, where the floods occur mainly in the September to November season, to the east, where the floods occur mainly in the period from autumn to late spring. The shift in seasonality is paralleled by a decreasing basin size and unit peak discharge from south-west to east. These findings are supported by the work of Parajka et al. (2010) who analysed the differences in the long-term regimes of extreme precipitation and floods across the Alpine-Carpathian range, and of~~

~~Dayan et al. (2015) who analysed the seasonality signal of atmospheric deep convection in the Mediterranean area.~~

~~We used the Budyko diagram (Budyko, 1974) to characterise the climatic context of the catchments included in the EuroMedeFF database (Figure 2). The Budyko framework plots the evaporation index (i.e., the ratio of mean annual actual evaporation to mean annual precipitation, AET/P) versus the aridity index (i.e., the ratio of mean annual potential evapotranspiration to mean annual precipitation PET/P). The mean values of these variables were calculated for each river basin, so the number of points plotted in Figure 2 is smaller than the total number of flash floods in the database. Figure 2 also reports the empirical Budyko curve (Budyko,1974), which fits well with the upper envelope of the data included in the data archive. Not surprisingly, the catchments under Arid or Arid-Mediterranean climate display typically water-limited conditions, with the aridity index, PET/P > 1. Continental, Alpine and Alpine-Mediterranean catchments lie in the energy-limited sector of the Budyko plot, with aridity index, PET/P < 1, indicating wet climate. Mediterranean catchments often display water-limited conditions, although less severe than catchments under Arid and Arid-Mediterranean climate.~~

Overall, 680 peak discharge data are included in the archive: 32% (219) were recorded by river gauging stations ~~and~~ or based on data from reservoir operations, and 68% (461) from IPEC surveys. We followed the geomorphic impact-based linear error analysis of the slope conveyance discharge determination presented in Amponsah et al. (2016) for the uncertainty assessment of the IPEC peak flood estimates. Table 2 reports the number of river sections for each of the climatic regions and the corresponding summary statistics of the upstream drainage area. Almost 90% of the included discharge data are from the Mediterranean region, which is consistent with ~~the higher occurrence of high-intensity~~ increasing collation and analysis of flash ~~floods~~ flood data in this region compared to other climatic regions in Europe (e.g., Gaume et al., 2009; Marchi et al., 2010). The area of the basins included in the archive ranges from 0.27 to 2586 km^2. Table 2 shows that flash flooding may impact larger basins in the Mediterranean, Alpine and Arid regions than those considered in the Inland Continental region. This support earlier findings from Gaume et al. (2009).

Table 3 reports summary statistics of the upstream drainage area for the two discharge assessment methods (stream gauges and indirect methods). As expected, stream gauges correspond to larger areas whereas post-flood surveys play major roles in documenting peak discharges for smaller drainage areas (Borga et al., 2008; Marchi et al., 2010; Amponsah et al., 2016). Nevertheless, the database also includes discharge data from a few measuring stations deployed in small research catchments. This allows to ~~decrease~~ reduce the uncertainty related to the estimation of peak discharge in very small catchments (Braud et al., 2014).

The relationship between the unit peak discharge (i.e., peak discharge normalized by the upstream drainage area) and the upstream area was investigated for the EuroMedeFF database to identify the control exerted by catchment size on flood peaks (Figure 3) and to analyse its variation among the main four climatic regions (Figures 4a-d). Not surprisingly, the unit peak discharges exhibit a marked dependence on watershed area. The envelope curve, representing the observed upper limit of the relationship, was empirically derived as a power-law function for all the floods as well as for the four different main climate region. The envelope curve representative for all the floods is similar in shape to that reported by Gaume et al. (2009) and Marchi et al. (2010) in previous analyses in the same hydro-climatic context. However, the multiplier reported here is larger than that reported in earlier analyses, due to the inclusion of recent more intense cases documented in large catchments. Inspection of the multiplier and exponent coefficients of the envelope curves reveals that the same exponent provides a good fit for the different climatic regions, whereas the highest multiplier is reported for the Mediterranean region, with an intermediate value for the Alpine-Mediterranean and Alpine basins, and the same lowest value for Inland Continental, Arid-Mediterranean and Arid basins. For small basin areas (1 to 5 km^2), Mediterranean and Alpine catchments are shown to experience similar extreme peaks.

Figures 5a-b shows the relationship between unit peak discharge based on the two discharge assessment methods and watershed area in a log-log diagram, together with the envelope curves. Indirect estimates of peak discharges show similar dependence of unit peak discharge on catchment size as that reported in Figure 3, showing that the information content of the overall envelope curve is dominated by the flood obtained based on post flood campaigns. Indeed, peak data from stream gauging stations, show a clearly different exponent of the envelope curve (-0.12) if compared to post-flood indirect peak flow estimates (and to the ones previously shown in Figure 3). The highest values of the peak discharge are often missed by the gauging stations because of insufficient density of stream gauge networks and/or damage to the stations during ~~the~~ floods. This sampling problem is more severe in small basins: as a consequence, both the value of the multiplier and the exponent of the envelope equation are lower in Figure 5a than in the plots that include post-flood peak discharge estimation in ungauged streams (Figures 3 and 5b).

Conclusions

We presented an observational dataset that provides integrated fine resolution data for high intensity flash floods that occurred in Europe and in the Mediterranean region from 1991 to 2015. The dataset is based on a unique collection of rainfall and discharge data (including data from post-flood surveys) for basins ranging in size from 0.27 to 2586 km^2. The archive provides high-resolution data enabling a number of flash flood ~~analysis~~analyses. It allows the analysis of the space-time distribution of causative rainfall, which may be used to investigate methodologies for rainfall downscaling. The data may foster the investigation of the rainfall-runoff relationship at multiple sites within the flash flood environment. This may lead~~s~~ to the identification of possible thresholds in runoff generation which may be related to initial conditions, rainfall rates and accumulations, and catchment properties. Moreover, it allows investigations to clarify the dependence existing between spatial rainfall organisation, basin morphology and runoff response. ~~Finally, t~~The archive may be used as a benchmark for the assessment of hydrological models and flash flood forecasting procedures in various hydro-climatic settings. The availability of fine resolution rainfall data may be used to better understand how rainfall spatial and temporal variability must be considered in hydrological models for accurate prediction of flash flood response. Furthermore, the availability of multiple flash flood response data along the river network may be exploited to better understand how calibration of hydrological models may be transferred across events and sites characterised by different severity.

Finally, inspection of the data included in the archive shows the relevance that indirect peak flow estimates have in flash flood analysis, particularly for small basins. This shows the urgency of developing standardised methods for post-flood surveys in order to gather flood response data, including flow types, flood peak magnitude and time, damages, and social response. This is key to further advance understanding of the causative processes and improve assessment of both flash flood hazard and vulnerability aspects (Calianno et al., 2013; Ruin et al., 2014).

Data availability

The EuroMedeFF dataset is publicly available and can be downloaded from http://mistrals.sedoo.fr/?editDatsId=1493&datsId=1493&project_name=HyMeX&q=euromedeff. The dataset is also made available with the following unique DOI provided by the HyMeX database administrators: https://doi.org/10.6096/MISTRALS-HyMeX.1493.

Team list

William Amponsah (WA); Pierre-Alain Ayral (P-AA); Brice Boudevillain (BB); Christophe Bouvier (CB); Isabelle Braud (IB); Pascal Brunet (PB); Guy Delrieu (GD); Jean-François Didon-Lescot (J-FD-L); Eric Gaume (EG); Laurent Lebouc (LL); Lorenzo Marchi (LM); Francesco Marra (FM); Efrat Morin (EM); Guillaume Nord (GN); Olivier Payrastre (OP); Davide Zoccatelli (DZ) and Marco Borga (MB).

Author contributions

Compilation of the flash flood data from Italy, Germany, Slovenia and Romania were done by WA, LM, DZ and MB. The Israeli data were compiled by EM and FM, whereas the French data were compiled by IB and OP, with contributions from P-AA, BB, CB, PB, GD, J-FD-L, EG, LL and GN. The initial draft of the paper was written by WA with the contributions of MB for Sections 1 and 5; EM, FM, LM, IB, OP, GD, EG, DZ and MB for Sections 2 and ~~4~~3, FM for Section ~~3~~4.1, and LM for Section ~~3~~4.2. All authors contributed through their revision of the text.

Competing interests

The authors declare that they have no conflict of interest.

Acknowledgements

This paper contributes to the HyMeX program (www.hymex.org). Collation of hydrometeorological data and processing of data collated through post flood surveys for the Italian events have been done in the framework of the Next-Data Project (Italian Ministry of University and Research and National Research Council of Italy - CNR). Part of the data was acquired through the Hydrometeorological Data Resources and Technologies for Effective Flash Flood Forecasting (HYDRATE) project (European Commission, Sixth Framework Programme, Contract 037024). Part of the data provided in this data set was acquired during the FloodScale project, funded by the French National Research Agency (ANR) under contract n° ANR 2011 BS56 027. We also benefited from funding by the MISTRALS/HyMeX program (http://www.mistrals-home.org), in particular for post-flood surveys. The rainfall reanalysis for the French events were provided by the OHM-CV observatory (observation service supported by the Institut National des Sciences de l'Univers, section Surface et Interfaces Continentales and the Observatoire des Sciences de l'Univers de Grenoble). We thank Arthur Hamburger which work was supported by the Labex OSUG@2020 (Investissements d'avenir – ANR10 LABX56) and the SCHAPI. We also thank SCHAPI, EDF-DTG for providing some of the French stream gauge discharge data, and Meteo France for providing French raingauge and radar input data. For Israel, raw radar data were obtained from E.M.S (Mekorot company), rain gauge data from the Israel Meteorological Service, streamgauge data from the Israel Hydrological Service, and post-flood estimates from reports by the Soil Erosion Research Station at the Ministry of Agriculture and Rural Development. The HyMeX database teams (ESPRI/IPSL and SEDOO/Observatoire Midi-Pyrénées) helped in making the data set available on the HyMeX database.

References

Adamovic, M., Branger, F., Braud, I., Kralisch, S., 2016. Development of a data-driven semi-distributed hydrological model for regional scale catchments prone to Mediterranean flash floods. J. Hydrol., 541, Part A: 173-189.

Amponsah, W., Marchi, L., Zoccatelli, D., Boni, G., Cavalli, M., Comiti, F., Crema, S., Lucía, A., Marra, F., Borga, M., 2016. Hydrometeorological characterisation of a flash flood associated with major geomorphic effects: Assessment of peak discharge uncertainties and analysis of the runoff response. J. Hydrometeor,, 17, 3063-3077.

Borga, M., Boscolo, P., Zanon, F., Sangati, M., 2007. Hydrometeorological Analysis of the 29 August 2003 Flash Flood in the Eastern Italian Alps. J. Hydrometeor., 8, 1049–1067.

Borga, M., Gaume, E., Creutin, J.D., Marchi, L., 2008. Surveying flash flood response: gauging the ungauged extremes., Hydrol. Processes, 22, 3883–3885.

Borga M., Stoffel, M., Marchi, L., Marra, F., Jacob, M., 2014. Hydrogeomorphic response to extreme rainfall in headwater systems: flash floods and debris flows. Journal of Hydrology, 518, 194–205. http://doi.org/10.1016/j.jhydrol.2014.05.022

Boudevillain, B., Delrieu, G., Wijbrans, A., Confoland, A., 2016. A high-resolution rainfall re-analysis based on radar–raingauge merging in the Cévennes-Vivarais region, France. J. Hydrol., 541, Part A: 14-23.

Bouilloud, L., Delrieu, G., Boudevillain, B., Borga, M., Zanon, F. 2009. Radar rainfall estimation for the postevent analysis of a Slovenian flash-flood case: application of the Mountain Reference Technique at Cband frequency. Hydrol. Earth Syst. Sci., 13, 1349–1360.

Bouilloud, L., Delrieu, G., Boudevillain, B., Kirstetter, P.-E., 2010: Radar rainfall estimation in the context of post-event analysis of flash-flood events. J. Hydrol., 394 (1-2), 17-27.

Braud, I., and Co-authors, 2014. Multi-scale hydrometeorological observation and modelling for flash flood understanding. Hydrol. Earth Syst. Sci., 18(9): 3733-3761.

Braud, I., Borga, M., Gourley, J., Hürlimann, M., Zappa, M., Gallart, F., 2016. Flash floods, hydro-geomorphic response and risk management. J. Hydrol., 541: 1-5.

Brunet, P., Bouvier, C., 2017. Analysis of the September 12th 2015 Lodève (France) flash flood: influence of karsts on flood characteristics, La Houille Blanche, n° 3, 2017, p. 39-46.

Brunet, P., Bouvier, C., Neppel, L., 2018. Retour d'expérience sur les crues des 6 et 7 octobre 2014 à Montpellier-Grabels (Hérault, France): caractéristiques hydro-météorologiques et contexte historique de

l'épisodePhysio-Géo Géographie physique et environnement Volume 12 | 2018 Varia 2018 https://journals.openedition.org/physio-geo/5710
Budyko, M.I., 1974. Climate and Life. Academic Press, New York.
Calianno, M., Ruin, I., Gourley, J.J., 2013. Supplementing flash flood reports with impact classifications. Journal of Hydrology, 477, pp. 1-16.
Collier, C., 2007. Flash flood forecasting: What are the limits of predictability? Quarterly Journal of the Royal Meteorological Society 133 (622A), 3–23.
Dayan, U., Nissen, K., Ulbrich, U., 2015. Review Article: Atmospheric conditions inducing extreme precipitation over the eastern and western Mediterranean. Natural Hazards and Earth System Sciences, 15 (11), 2525-2544.
Delrieu, G, and Co-authors, 2005. The catastrophic flash-flood event of 8–9 September 2002 in the Gard region, France: a first case study for the Cévennes-Vivarais Mediterranean Hydro-meteorological Observatory. J. Hydrometeor., 6: 34–52.
Delrieu, G., Wijbrans, A., Boudevillain, B., Faure, D., Bonnifait, L., Kirstetter, P.-E., 2014. Geostatistical radar–raingauge merging: A novel method for the quantification of rain estimation accuracy. Advances in Water Resources, 71(0): 110-124.
Destro, E., Amponsah, W., Nikolopoulos, EI., Marchi, L., Marra, F., Zoccatelli, D., Borga, M., 2018. Coupled prediction of flash flood response and debris flow occurrence: Application on an alpine extreme flood event. J. Hydrol., 558, 225-237.
Destro, E., Marchi, L., Amponsah, W., Tarolli, P., Crema, S., Zoccatelli, D., Marra, F., Borga, M., 2016. Hydrological analysis of the flash flood event of August 2, 2014 in a small basin of the Venetian Prealps. Quaderni di Idronomia Montana, 34, 307-316 (in Italian, abstract in English).
Gaume, E. , Livet, M., Desbordes, M., Villeneuve, J.P., 2004. Hydrological analysis of the river Aude, France, flash flood on 12 and 13 November 1999, J. Hydrol., 286, 135–154.
Gaume, E., Borga, M., 2008. Post-flood field investigations in upland catchments after major flash floods: proposal of a methodology and illustrations. Journal of Flood Risk Management 1 (4): 175–189.
Gaume, E.V., and Co-authors, 2009. A collation of data on European flash floods. J. Hydrol., 367, 70–78.
Germann, U., Galli G., Boscacci M., and Bolliger M., 2006. "Radar Precipitation Measurement in a Mountainous Region." Quarterly Journal of the Royal Meteorological Society 132(618): 1669–92. http://doi.wiley.com/10.1256/qj.05.190
Greenbaum, N., Margalit, A., Schick, A.P., Sharon, D., Baker, V.R., 1998. A high magnitude storm and flood in a hyperarid catchment, Nahal Zin, Negev Desert, Israel. Hydrol. Processes, 12, 1-23.
Grodek, T., Jacoby, Y., Morin, E., Katz, O., 2012. Effectiveness of exceptional rainstorms on a small Mediterranean basin. Geomorphology, 159–160, 156-168.
Hardy, J., Gourley, J.J., Kirstetter, P.-E., Hong, Y., Kong, F., Flamig, Z.L., 2016. A method for probabilistic flash flood forecasting. J. Hydrol., 541, 480-494.
Le Bihan, G., Payrastre, O., Gaume, E., Moncoulon, D., and Pons, F.: The challenge of forecasting impacts of flash floods: test of a simplified hydraulic approach and validation based on insurance claim data, Hydrol. Earth Syst. Sci., 21, 5911-5928, https://doi.org/10.5194/hess-21-5911-2017, 2017.
Lange, J., Leibundgut, C., Greenbaum, N., Schick, A. P., 1999. A noncalibrated rainfall-runoff model for large, arid catchments. Water Resources Research, 35, 2161-2172.
Lumbroso, D., Gaume, E., 2012. Reducing the uncertainty in indirect estimates of extreme flash flood discharges. J. Hydrol., 414–415, 16–30.
Marchi, L., Borga, M., Preciso, E., Gaume, E., 2010. Characterisation of selected extreme flash floods in Europe and implications for flood risk management. J. Hydrol., 394, 118–133.
Marchi, L., Borga, M., Preciso, E., Sangati, M., Gaume, E., Bain, V., Delrieu, G., Bonnifait, L., Pogačnik, N., 2009. Comprehensive post-event survey of a flash flood in Western Slovenia: observation strategy and lessons learned. Hydrol. Processes, 23(26), 3761-3770.
Marchi, L., Cavalli, M., Amponsah, W., Borga, M., Crema, S., 2016. Upper limits of flash flood stream power in Europe. Geomorphology, 272, 68-77.
Marra, F, Morin, E, 2015. Use of radar QPE for the derivation of Intensity–Duration–Frequency curves in a range of climatic regimes. J. Hydrolo., 531 (2), 427-440.

Marra, F., Nikolopoulos, E.I., Creutin, J.D., Borga, M., 2014. Radar rainfall estimation for the identification of debris-flow occurrence thresholds. J. Hydrol., 519, 1607-1619.

Morin, E., Harats, N., Jacoby, Y., Arbel, S., Getker, M., Arazi, A., Grodek, T., Ziv, B., Dayan, U., 2007. Studying the extremes: Hydrometeorological investigation of a flood-causing rainstorm over Israel. Advances in Geosciences, 12, 107–114.

Morin, E., Jacoby, Y., Navon, S., Bet-Halachmi, E., 2009. Towards flash flood prediction in the dry Dead Sea region utilizing radar rainfall information. Advances in Water Resources, 32, 1066-1076.

Naulin J.P., Gaume E., Payrastre O., 2012. Distributed flood forecasting for the management of the road network in the Gard Region (France), Weather Radar and Hydrology, IAHS Publication, 351, 544-549.

Naulin J.P, Payrastre O., Gaume E., 2013. Spatially distributed flood forecasting in flash flood prone areas: Application to road network supervision in Southern France, Journal of Hydrology, 486, 88-99, https://doi.org/10.1016/j.jhydrol.2013.01.044.

Niedda M., Amponsah, W., Marchi, L., Zoccatelli, D., Marra, F., Crema, S., Pirastru, M., Marrosu, R., Borga, M., 2015. The cyclone Cleopatra of November 18, 2013 in Sardinia, event management, measurement and modelling. Quaderni di Idronomia Montana, 32/1, 47-58 (in Italian, abstract in English).

Norbiato, D., Borga, M., Dinale, R., 2009. Flash flood warning in ungauged basins by use of the Flash Flood Guidance and model-based runoff thresholds. Meteorological Applications 16 (1), 65–75.

Parajka, J., and Co-author, 2010. Seasonal characteristics of flood regimes across the Alpine-Carpathian range. J. Hydrol., 394(1-2): 78–89.

Payrastre, O., Gaume, E., Javelle, P., Janet, B., Fourmigué, P., Lefort, Ph., Martin, A., Boudevillain, B., Brunet, P., Delrieu, G., Marchi, L., Aubert, Y., Dautrey, E., Durand, L., Lang, M., Boissier, L., Douvinet, J., Martin, C., Ruin, I., 2012. Hydrological analysis of the catastrophic flash flood of 15th June 2010 in the area of Draguignan (Var, France)-TTO2D d'HYMEX, SHF conference "Evénements extremes Fluviaux et Maritimes", Paris, 1-2 février 2012.

Righini, M., Surian, N., Wohl, E.E., Marchi, L., Comiti, F., Amponsah, W., Borga, M., 2017. Geomorphic response to an extreme flood in two Mediterranean rivers (northeastern Sardinia, Italy): Analysis of controlling factors. Geomorphology, 290, 184-199.

Rozalis, S., Morin, E., Yair, Y., Price, C., 2010. Flash flood prediction using an uncalibrated hydrological model and radar rainfall data in a Mediterranean watershed under changing hydrological conditions. J. Hydrol., 394, 245–255.

Ruin, I., and Coauthors, 2014. Social and hydrological responses to extreme precipitations: An interdisciplinary strategy for postflood investigation. Weather, Climate, and Society, 6, 135-153.

Ruiz-Villanueva, V., Borga, M., Zoccatelli, D., Marchi, L., Gaume, E., Ehret, U., 2012. Extreme flood response to short-duration convective rainfall in South-West Germany. Hydrol. Earth Syst. Sci., 16, 1543–1559.

Saharia, M., Kirstetter, P.-E., Vergara, H., Gourley, J.J., Hong, Y., 2017. Characterization of floods in the United States. J. Hydrol., 548, 524-535.

Smith, B.K., Smith, J.A., 2015. The flashiest watersheds in the contiguous United States. J. Hydrometeor., 16 (6), 2365-2381.

Tarolli, P., Borga, M., Morin, E., Delrieu, G., 2012. Analysis of flash flood regimes in the North-Western and South-Eastern Mediterranean regions. Nat. Hazards Earth Syst. Sci., 12, 1255–1265.

Tramblay, Y., Bouvier, C., Martin, C., Didon-Lescot, J.F., Todorovik, D., Domergue, J.M., 2010. Assessment of initial soil moisture conditions for event-based rainfall–runoff modelling. J. Hydrol., 387, 176–187

Vannier, O., Anquetin, S., Braud, I., 2016. Investigating the role of geology in the hydrological response of Mediterranean catchments prone to flash-floods: Regional modelling study and process understanding. J. Hydrol., 541 (Part A), 158-172.

Villarini, G., Krajewski W.F., 2010. "Review of the Different Sources of Uncertainty in Single Polarization Radar-Based Estimates of Rainfall." Surveys in Geophysics 31(1): 107–29.

Yatheendradas, S., Wagener, T., Gupta, H., Unkrich, C., Goodrich, D., Schaffner, M., Stewart, A., 2008. Understanding uncertainty in distributed flash flood forecasting for semiarid regions. Water Resources Research, 44 (5), W05S19.

Zanon, F., Borga, M., Zoccatelli, D., Marchi, L., Gaume, E., Bonnifait, L., Delrieu, G., 2010. Hydrological analysis of a flash flood across a climatic and geologic gradient: the September18, 2007 event in Western Slovenia. J. Hydrol., 394, 182–197.
Zoccatelli, D., Borga, M., Zanon, F., Antonescu, B., Stancalie, G., 2010. Which rainfall spatial information for flash flood response modelling? A numerical investigation based on data from the Carpathian range, Romania. J. Hydrol., 394, 148–161.

TABLES

Table 1. Summary information on the flash flood database

	Event ID	Region/ catchment impacted (Country)	Date of flood peak	Climatic Region	No. of ~~studied watersheds~~ river sections (No. of stream gauges)	Range in Watershed area [km^2]	Storm duration [h]	Range of unit peak discharge [$m^3/s/km^2$]	Previous studies
1	ORBIEL1999	Orbiel (France)	13.11.1999	Mediterranean	21 (1)	2.5 – 239	29	0.80 – 13.00	Gaume et al., 2004
2	NIELLE1999	Nielle (France)	13.11.1999	Mediterranean	16 (0)	5 – 125	33	6.00 – 20.00	Gaume et al., 2004
3	VERDOUBLE1999	Verdouble (France)	13.11.1999	Mediterranean	29 (1)	0.35 – 350	30	1.30 – 77.14	Gaume et al., 2004
4	VIDOURLE2002	Vidourle (France)	09.09.2002	Mediterranean	25 (2)	13 – 110	26	1.33 – 22.22	Delrieu et al., 2005
5	GARDONS2002	Gardons (France)	08.09.2002	Mediterranean	66 (6)	1.6 – 1855	25	1.99 – 50.00	Delrieu et al., 2005
6	CEZE2002	Ceze (France)	08.09.2002	Mediterranean	12 (4)	7.3 – 1120	25	0.94 – 19.18	Delrieu et al., 2005
7	VALESCURE2006	Valescure (France)	19.10.2006	Mediterranean	4 (4)	0.27 – 3.93	34	2.31 – 6.94	Tramblay et al., 2010
8	GARDONS2008	Gardons (France)	21.10.2008	Mediterranean	33 (9)	0.27 – 1521	21	0.68 – 34.55	Naulin et al., 2012,2013 ; Vannier et al., 2016
9	CEZE2008	Ceze (France)	21.10.2008	Mediterranean	21 (3)	0.95 – 1120	21	0.71 – 22.16	Naulin et al., 2012,2013 ;
10	ARGENS2010	Argens (France)	15.06.2010	Mediterranean	35 (1)	3 – 2550	23	0.73 – 10.00	Payrastre et al., 2012 ; Le Bihan et al., 2017
11	ARDECHE2011	Ardeche (France)	3&4.11. 2011	Mediterranean	14 (14)	16 – 2263	31	0.66 – 9.88	Adamovic et al., 2016
12	ARDECHE2013	Ardeche (France)	23.10. 2013	Mediterranean	15 (14)	2.2 – 2263	17	0.70 – 8.18	
13	ORB2014	Orb (France)	17.09.2014	Mediterranean	7 (3)	3.5 – 335	11	2.08 – 20.31	
14	VIDOURLE2014	Vidourle (France)	18.09.2014	Mediterranean	8 (3)	15 – 770	18	0.89 – 17.67	

15	HERAULT2014	Herault (France)	17.09.2014	Mediterranean	10 (4)	1 – 1305	29	1.08 – 23.00	
16	GARDONS2014-A	Gardons (France)	18& 20.09.2014	Mediterranean	28 (21)	0.27 – 1855	18	0.63 – 26.67	
17	ARDECHE2014-A	Ardeche (France)	19.09.2014	Mediterranean	16 (15)	3.4 – 2263	13	0.98 – 12.85	
18	ARDECHE2014-B	Ardeche (France)	10&11.10. 2014	Mediterranean	17 (15)	3.4 – 2263	41	0.54 – 2.92	
19	LEZMOSSON2014	Lez Mosson (France)	07.10.2014	Mediterranean	20 (4)	0.38 – 306	7	0.76 – 46.15	Brunet et al., 2014
20	GARDONS2014-B	Gardons (France)	10.10.2014	Mediterranean	30 (13)	0.27 – 1855	29	0.81 – 22.37	
21	CEZE2014	Ceze (France)	11.10. 2014	Mediterranean	6 (3)	77 – 1120	15	1.04 – 7.14	
22	ARDECHE2014-C	Ardeche (France)	3&4.11. 2014	Mediterranean	16 (16)	3.4 – 2263	15	0.77 – 7.45	
23	ARDECHE2014-D	Ardeche (France)	14&15.11. 2014	Mediterranean	14 (14)	3.4 – 2263	16	0.97 – 2.47	
24	ARDECHE2014-E	Ardeche (France)	27.11.2014	Mediterranean	12 (12)	3.4 – 2263	7	0.54 – 0.99	
25	LERGUE2015	Lergue (France)	12.09.2015	Mediterranean	11 (3)	7.5 – 1850	21	0.68 – 20.50	Brunet and Bouvier, 2017
26	VALESCURE2015-A	Valescure (France)	12.09.2015	Mediterranean	4 (4)	0.27 – 3.93	26	0.87 – 4.38	Tramblay et al., 2010
27	ARGENTIERE2015	Argentiere (France)	03.10.2015	Mediterranean	14 (0)	1.3 – 29	6	4.45 – 18.21	
28	BRAGUE2015	Brague (France)	03.10.2015	Mediterranean	16 (0)	0.6 – 41.5	6	3.03 – 23.43	
29	FRAYERE2015	Frayere (France)	03.10.2015	Mediterranean	6 (0)	1.3 – 21.4	6	4.44 – 18.25	
30	VALESCURE2015-B	Valescure (France)	28.10.2015	Mediterranean	3 (3)	0.27 – 3.93	38	1.33 – 22.22	Tramblay et al., 2010
31	ZIN1991	Zin (Israel)	13.10.1991	Arid	1 (1)	233.5	3	2.28	Greenbaum et al., 1998; Lange et al., 1999; ~~Tarolli et al~~Tarolli et al., 2012~~, 2012~~
32	NEQAROT1993	Neqarot (Israel)	23.12.1993	Arid	1 (1)	699.5	4	1.00	Tarolli et al., 2012
33	NORTHDEADSEA1994	Teqoa (Israel)	05.11.1994	Arid-Mediterranean	1 (1)	142	4	1.12	Tarolli et al., 2012
34	NORTHDEADSEA2001	Darga, Arugot (Israel)	02.05.2001	Arid-Mediterranean	2 (2)	235-70	4	0.82 – 1.78	Morin et al., 2009; Tarolli et al., 2012

35	RAMOTMENASHE2006	Taninim, Qishon (Israel)	02.04.2006	Mediterranean	11 (0)	0.75 – 22	8	2.29 – 29.33	Morin et al., 2007; Grodek at al., 2012
36	HAROD2006	Harod (Israel)	27&28.10.2006	Mediterranean	12 (1)	1.2 – 100	5	0.58 – 10.00	Rozalis et al., 2010; Tarolli et al., 2012
37	QUMERAN2007	Qumeran (Israel)	12.05.2007	Arid	5 (0)	8.5 – 45.3	3	3.35 – 12.96	Rozalis et al., 2010; Tarolli et al., 2012-
38	STARZEL2008	Starzel (Germany)	02.06.2008	Continental	17 (0)	1 – 119.5	8	0.81 – 11.74	Ruiz-Villanueva et al., 2012
39	SORA2007	Selška Sora (Slovenia)	18.09.2007	Alpine-Mediterranean	18 (2)	1.9 – 212	16.5	1.58 – 10.85	Zanon et al., 2010
40	FEERNIC2005	Feernic (Romania)	23.08.2005	Continental	1 (1)	168	5.5	2.22	Zoccatelli et al., 2010
41	CLIT2006	Clit (Romania)	30.06.2006	Continental	1 (0)	36	4	4.86	Zoccatelli et al., 2010
42	GRINTIES2007	Grinties (Romania)	04.08.2007	Continental	1 (0)	52	4	1.92	Zoccatelli et al., 2010
43	SESIA2002	Sesia (Italy)	05.06.2002	Alpine-Mediterranean	6 (6)	75 – 2586	22	1.33 – 4.78	
44	FELLA2003	Fella (Italy)	29.08.2003	Alpine-Mediterranean	7 (5)	24 – 623	12	0.52 – 8.37	Borga et al., 2007
45	ISARCO2006	Isarco and Passirio (Italy)	3&4.10.2006	Alpine	2 (2)	48 – 75	12.5	0.75 – 1.07	Norbiato et al., 2009
46	MAGRA2011	Magra (Italy)	25.10.2011	Mediterranean	36 (3)	0.5 – 936	24	1.70 – 28.19	Amponsah et al., 2016
47	VIZZE2012	Vizze (Italy)	04.08.2012	Alpine	3 (1)	45 – 108	18	0.93 – 1.55	Destro et al., 2018
48	SARDINIA2013	Cedrino-Posada (Italy)	18.11.2013	Mediterranean	18 (1)	4 – 627	12	4.98 – 25.64	Niedda et al., 2015; Righini et al., 2017
49	LIERZA2014	Lierza (Italy)	02.08.2014	Alpine-Mediterranean	8 (0)	1.5 – 12.4	1.5	12.03 – 27.59	Destro et al., 2016

~~**Table 1.** Summary information on the flash flood database~~

	~~Event ID~~	~~Region/ catchment impacted (Country)~~	~~Date of flood peak~~	~~Climatic Region~~	~~No. of studied watersheds (No. of stream gauges)~~	~~Range in Watershed area [km^2]~~	~~Storm duration [h]~~		~~Previous studies~~

~~1~~	~~ORBIEL1999~~	~~Orbiel (France)~~	~~13.11.1999~~	~~Mediterranean~~	~~21 (1)~~	~~2.5 – 239~~	~~29~~		~~Gaume et al. 2004~~
~~2~~	~~NIELLE1999~~	~~Nielle (France)~~	~~13.11.1999~~	~~Mediterranean~~	~~16 (0)~~	~~5 – 125~~	~~33~~		~~Gaume et al. 2004~~
~~3~~	~~VERDOUBLE1999~~	~~Verdouble (France)~~	~~13.11.1999~~	~~Mediterranean~~	~~29 (1)~~	~~0.35 – 350~~	~~30~~		~~Gaume et al. 2004~~
~~4~~	~~VIDOURLE2002~~	~~Vidourle (France)~~	~~09.09.2002~~	~~Mediterranean~~	~~25 (2)~~	~~13 – 110~~	~~26~~		~~Delrieu et al 2005~~
~~5~~	~~GARDONS2002~~	~~Gardons (France)~~	~~08.09.2002~~	~~Mediterranean~~	~~66 (6)~~	~~1.6 – 1855~~	~~25~~		~~Delrieu et al 2005~~
~~6~~	~~CEZE2002~~	~~Ceze (France)~~	~~08.09.2002~~	~~Mediterranean~~	~~12 (4)~~	~~7.3 – 1120~~	~~25~~		~~Delrieu et al 2005~~
~~7~~	~~VALESCURE2006~~	~~Valescure (France)~~	~~19.10.2006~~	~~Mediterranean~~	~~4 (4)~~	~~0.27 – 3.93~~	~~34~~		~~Tramblay et al., 2010~~
~~8~~	~~GARDONS2008~~	~~Gardons (France)~~	~~21.10.2008~~	~~Mediterranean~~	~~33 (9)~~	~~0.27 – 1521~~	~~21~~		~~Naulin et al. 2012,2013 ; Vannier et al., 2016~~
~~9~~	~~CEZE2008~~	~~Ceze (France)~~	~~21.10.2008~~	~~Mediterranean~~	~~21 (3)~~	~~0.95 – 1120~~	~~21~~		~~Naulin et al. 2012,2013 ;~~
~~10~~	~~ARGENS2010~~	~~Argens (France)~~	~~15.06.2010~~	~~Mediterranean~~	~~35 (1)~~	~~3 – 2550~~	~~23~~		~~Payrastre et al., 2012 ; Le Bihan et al., 2017~~
~~11~~	~~ARDECHE2011~~	~~Ardeche (France)~~	~~3&4.11. 2011~~	~~Mediterranean~~	~~14 (14)~~	~~16 – 2263~~	~~31~~		~~Adamovic et al., 2016~~
~~12~~	~~ARDECHE2013~~	~~Ardeche (France)~~	~~23.10. 2013~~	~~Mediterranean~~	~~15 (14)~~	~~2.2 – 2263~~	~~17~~		
~~13~~	~~ORB2014~~	~~Orb (France)~~	~~17.09.2014~~	~~Mediterranean~~	~~7 (3)~~	~~3.5 – 335~~	~~11~~		
~~14~~	~~VIDOURLE2014~~	~~Vidourle (France)~~	~~18.09.2014~~	~~Mediterranean~~	~~8 (3)~~	~~15 – 770~~	~~18~~		
~~15~~	~~HERAULT2014~~	~~Herault (France)~~	~~17.09.2014~~	~~Mediterranean~~	~~10 (4)~~	~~1 – 1305~~	~~29~~		
~~16~~	~~GARDONS2014-A~~	~~Gardons (France)~~	~~18& 20.09.2014~~	~~Mediterranean~~	~~28 (21)~~	~~0.27 – 1855~~	~~18~~		
~~17~~	~~ARDECHE2014-A~~	~~Ardeche (France)~~	~~19.09.2014~~	~~Mediterranean~~	~~16 (15)~~	~~3.4 – 2263~~	~~13~~		
~~18~~	~~ARDECHE2014-B~~	~~Ardeche (France)~~	~~10&11.10. 2014~~	~~Mediterranean~~	~~17 (15)~~	~~3.4 – 2263~~	~~41~~		
~~19~~	~~LEZMOSSON2014~~	~~Lez Mosson (France)~~	~~07.10.2014~~	~~Mediterranean~~	~~20 (4)~~	~~0.38 – 306~~	~~7~~		
~~20~~	~~GARDONS2014-B~~	~~Gardons (France)~~	~~10.10.2014~~	~~Mediterranean~~	~~30 (13)~~	~~0.27 – 1855~~	~~29~~		
~~21~~	~~CEZE2014~~	~~Ceze (France)~~	~~11.10. 2014~~	~~Mediterranean~~	~~6 (3)~~	~~77 – 1120~~	~~15~~		
~~22~~	~~ARDECHE2014-C~~	~~Ardeche (France)~~	~~3&4.11. 2014~~	~~Mediterranean~~	~~16 (16)~~	~~3.4 – 2263~~	~~15~~		

~~23~~	~~ARDECHE2014-D~~	~~Ardeche (France)~~	~~14&15.11.2014~~	~~Mediterranean~~	~~14 (14)~~	~~3.4 – 2263~~	~~16~~		
~~24~~	~~ARDECHE2014-E~~	~~Ardeche (France)~~	~~27.11.2014~~	~~Mediterranean~~	~~12 (12)~~	~~3.4 – 2263~~	~~7~~		
~~25~~	~~LERGUE2015~~	~~Lergue (France)~~	~~12.09.2015~~	~~Mediterranean~~	~~11 (3)~~	~~7.5 – 1850~~	~~21~~		~~Brunet and Bouvier, 2017~~
~~26~~	~~VALESCURE2015-A~~	~~Valescure (France)~~	~~12.09.2015~~	~~Mediterranean~~	~~4 (4)~~	~~0.27 – 3.93~~	~~26~~		~~Tramblay et al., 2010~~
~~27~~	~~ARGENTIERE2015~~	~~Argentiere (France)~~	~~03.10.2015~~	~~Mediterranean~~	~~14 (0)~~	~~1.3 – 29~~	~~6~~		
~~28~~	~~BRAGUE2015~~	~~Brague (France)~~	~~03.10.2015~~	~~Mediterranean~~	~~16 (0)~~	~~0.6 – 41.5~~	~~6~~		
~~29~~	~~FRAYERE2015~~	~~Frayere (France)~~	~~03.10.2015~~	~~Mediterranean~~	~~6 (0)~~	~~1.3 – 21.4~~	~~6~~		
~~30~~	~~VALESCURE2015-B~~	~~Valescure (France)~~	~~28.10.2015~~	~~Mediterranean~~	~~3 (3)~~	~~0.27 – 3.93~~	~~38~~		~~Tramblay et al., 2010~~
~~31~~	~~ZIN1991~~	~~Zin (Israel)~~	~~13.10.1991~~	~~Arid~~	~~1 (1)~~	~~233.5~~	~~3~~		~~Greenbaum et al., 1998; Lange et al., 1999; ,.Tarolli et a 2012~~
~~32~~	~~NEQAROT1993~~	~~Neqarot (Israel)~~	~~23.12.1993~~	~~Arid~~	~~1 (1)~~	~~699.5~~	~~4~~		~~Tarolli et al., 2012~~
~~33~~	~~NORTHDEADSEA1994~~	~~Teqoa (Israel)~~	~~05.11.1994~~	~~Arid-Mediterranean~~	~~1 (1)~~	~~142~~	~~4~~		~~Tarolli et al., 2012~~
~~34~~	~~NORTHDEADSEA2001~~	~~Darga, Arugot (Israel)~~	~~02.05.2001~~	~~Arid-Mediterranean~~	~~2 (2)~~	~~235-70~~	~~4~~		~~Morin et al., 2009; Taroll et al., 2012~~
~~35~~	~~RAMOTMENASHE2006~~	~~Taninim, Qishon (Israel)~~	~~02.04.2006~~	~~Mediterranean~~	~~11 (0)~~	~~0.75 – 22~~	~~8~~		~~Morin et al., 2007; Grode at al., 2012~~
~~36~~	~~HAROD2006~~	~~Harod (Israel)~~	~~27&28.10.2006~~	~~Mediterranean~~	~~12 (1)~~	~~1.2 – 100~~	~~5~~		~~Rozalis et al 2010; Taroll et al., 2012~~
~~37~~	~~QUMERAN2007~~	~~Qumeran (Israel)~~	~~12.05.2007~~	~~Arid~~	~~5 (0)~~	~~8.5 – 45.3~~	~~3~~		~~-~~
~~38~~	~~STARZEL2008~~	~~Starzel (Germany)~~	~~02.06.2008~~	~~Continental~~	~~17 (0)~~	~~1 – 119.5~~	~~8~~		~~Ruiz-Villanueva e al., 2012~~
~~39~~	~~SORA2007~~	~~Selška Sora (Slovenia)~~	~~18.09.2007~~	~~Alpine-Mediterranean~~	~~18 (2)~~	~~1.9 – 212~~	~~16.5~~		~~Zanon et al., 2010~~
~~40~~	~~FEERNIC2005~~	~~Feernic (Romania)~~	~~23.08.2005~~	~~Continental~~	~~1 (1)~~	~~168~~	~~5.5~~		~~Zoccatelli et al., 2010~~
~~41~~	~~CLIT2006~~	~~Clit (Romania)~~	~~30.06.2006~~	~~Continental~~	~~1 (0)~~	~~36~~	~~4~~		~~Zoccatelli et al., 2010~~
~~42~~	~~GRINTIES2007~~	~~Grinties (Romania)~~	~~04.08.2007~~	~~Continental~~	~~1 (0)~~	~~52~~	~~4~~		~~Zoccatelli et al., 2010~~

~~43~~	~~SESIA2002~~	~~Sesia (Italy)~~	~~05.06.2002~~	~~Alpine-Mediterranean~~	~~6 (6)~~	~~75 – 2586~~	~~22~~		
~~44~~	~~FELLA2003~~	~~Fella (Italy)~~	~~29.08.2003~~	~~Alpine-Mediterranean~~	~~7 (5)~~	~~24 – 623~~	~~12~~		~~Borga et al., 2007~~
~~45~~	~~ISARCO2006~~	~~Isarco and Passirio (Italy)~~	~~3&4.10. 2006~~	~~Alpine~~	~~2 (2)~~	~~48 – 75~~	~~12.5~~		~~Norbiato et al., 2009~~
~~46~~	~~MAGRA2011~~	~~Magra (Italy)~~	~~25.10.2011~~	~~Mediterranean~~	~~36 (3)~~	~~0.5 – 936~~	~~24~~		~~Amponsah e al., 2016~~
~~47~~	~~VIZZE2012~~	~~Vizze (Italy)~~	~~04.08.2012~~	~~Alpine~~	~~3 (1)~~	~~45 – 108~~	~~18~~		~~Destro et al., 2018~~
~~48~~	~~SARDINIA2013~~	~~Cedrino-Posada (Italy)~~	~~18.11.2013~~	~~Mediterranean~~	~~18 (1)~~	~~4 – 627~~	~~12~~		~~Niedda et al. 2015; Righin et al., 2017~~
~~49~~	~~LIERZA2014~~	~~Lierza (Italy)~~	~~02.08.2014~~	~~Alpine-Mediterranean~~	~~8 (0)~~	~~1.5 – 12.4~~	~~1.5~~		~~Destro et al., 2016~~

Table 2. Summary statistics for drainage areas for the EuroMedeFF database under different climatic regions

Climatic regions	No. of cases	Mean drainage area [km^2]	~~Standard deviation~~	25th – 75th quantiles [km^2]
Mediterranean	606	181	~~417.5~~	7.5 – 113.7
Alpine and Alpine-Mediterranean	44	150	~~415.0~~	8.6 – 97.2
Inland Continental	20	37.6	~~43.3~~	2.2 – 48.6
Arid and Arid-Mediterranean	10	148	~~216.5~~	13.5 – 210.7

Table 3. Summary statistics for drainage areas for the EuroMedeFF database based on the two classes of discharge assessment (stream gauges *vs* indirect methods)

Discharge assessment method	No. of cases	Mean drainage area [km^2]	~~Standard deviation~~	25th – 75th quantiles [km^2]
Stream gauges	219	438	~~616~~	60 – 543
Indirect methods (IPEC~~S~~)	461	49	~~135~~	6 – 45

FIGURE CAPTION

Figure 1: Location of the flash floods in Central and Western Mediterranean, the Alps, and Inland Continental Europe; inset is Eastern Mediterranean (Israel). The length of the arrow represents the area of the largest basin. Colour indicates the magnitude of the largest unit peak discharge. Direction represents the timing of the flash flood occurrence.

Figure 2: Budyko plot for the study basins (P: mean annual precipitation, AET: mean annual actual evapotranspiration, PET: mean annual potential evapotranspiration). In case of multiple nested catchments, only data for the largest one are reported.

Figure 3: Unit peak discharges versus drainage areas for the studied flash floods. The envelope curve for upper limit of the relationship is reported.

Figure 4: Unit peak discharges versus drainage areas based on climatic regions: (a) Mediterranean catchments, (b) Alpine-Mediterranean and Alpine catchments, (c) Inland Continental, and (d) Arid and Arid-Mediterranean catchments. The envelope curve for each climatic region is reported.

Figure 5: Unit peak discharges versus drainage areas based on discharge assessment methods: (a) stream gauges and (b) indirect methods. The envelope curves for the upper limits for each method are reported.

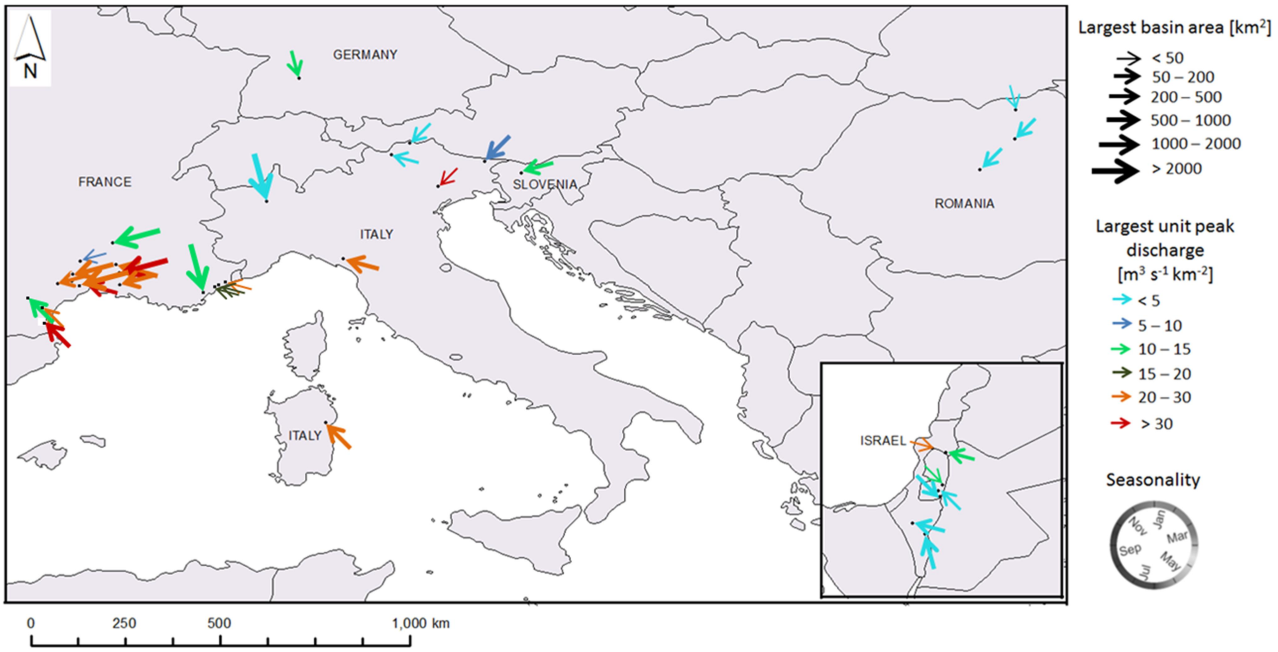

N
GERMANY
FRANCE
SLOVENIA
ROMANIA
ITALY
ITALY
ISRAEL
0
250
500
1,000 km
Largest basin area [km^2]
< 50
50 – 200
200 – 500
500 – 1000
1000 – 2000
> 2000
Largest unit peak discharge [m^3 s^{-1} km^{-2}]
< 5
5 – 10
10 – 15
15 – 20
20 – 30
> 30
Seasonality
Jan
Mar
May
Jul
Sep
Nov

Figure 1

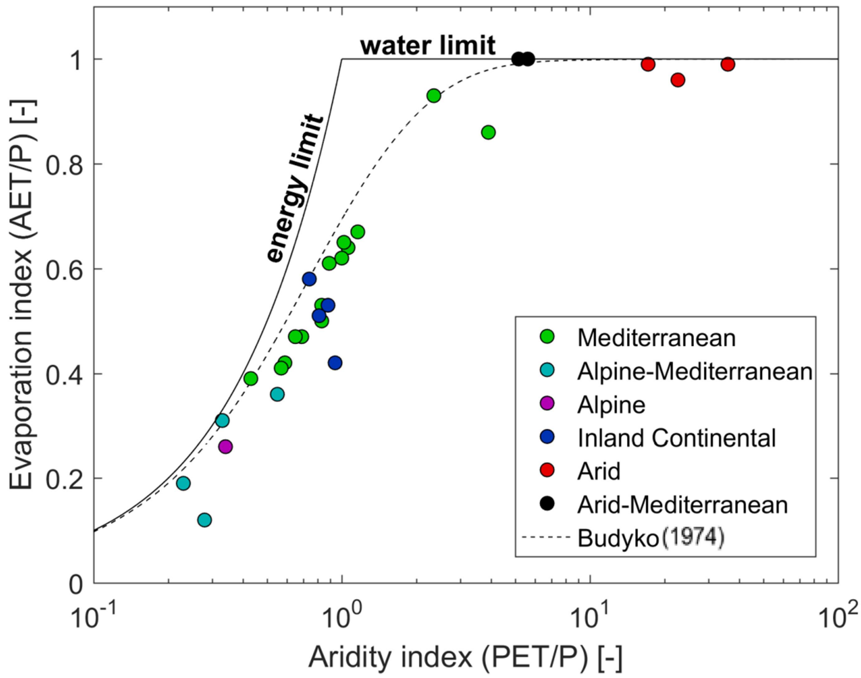
water limit
energy limit
Evaporation index (AET/P) [-]
Aridity index (PET/P) [-]
0
0.2
0.4
0.6
0.8
1
10^{-1}
10^{0}
10^{1}
10^{2}
Mediterranean
Alpine-Mediterranean
Alpine
Inland Continental
Arid
Arid-Mediterranean
Budyko (1974)

Figure 2

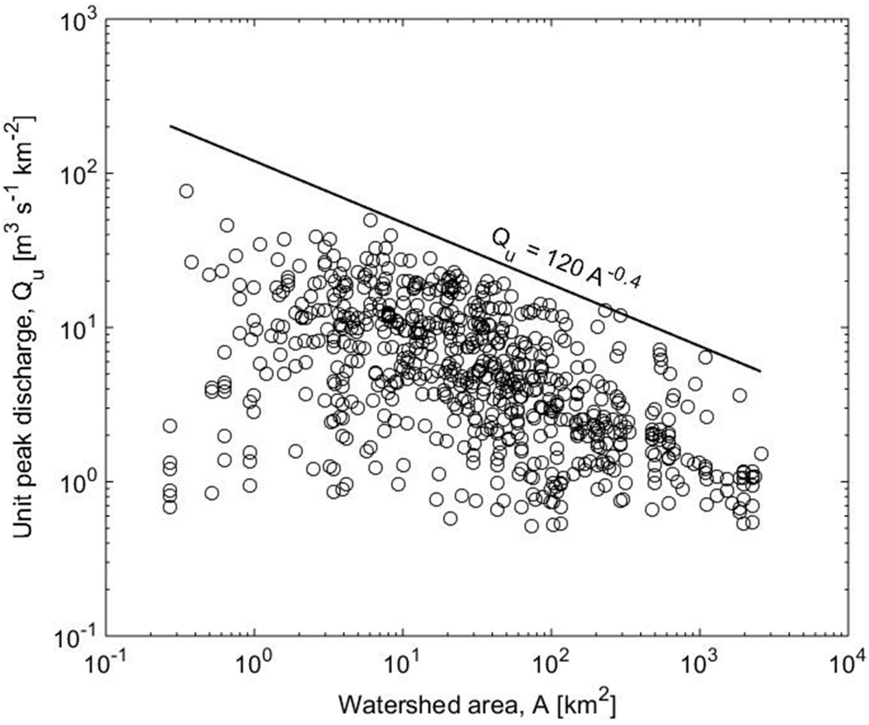

694

695 **Figure 3**

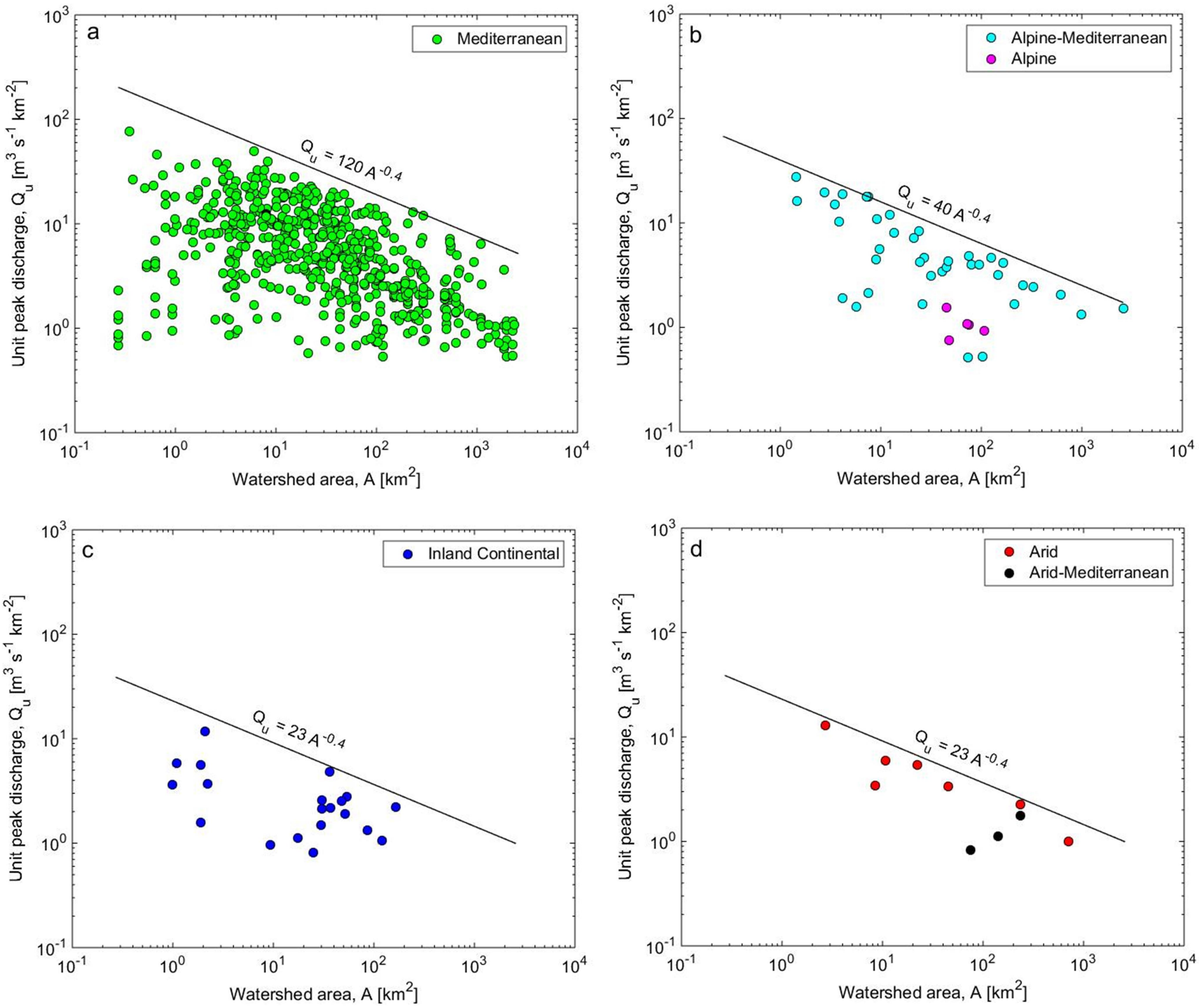
a
Mediterranean
$Q_u = 120\,A^{-0.4}$
b
Alpine-Mediterranean
Alpine
$Q_u = 40\,A^{-0.4}$
c
Inland Continental
$Q_u = 23\,A^{-0.4}$
d
Arid
Arid-Mediterranean
$Q_u = 23\,A^{-0.4}$
Unit peak discharge, Q_u [$m^3\,s^{-1}\,km^{-2}$]
Watershed area, A [km^2]
10^{-1}
10^{0}
10^{1}
10^{2}
10^{3}
10^{4}

Figure 4

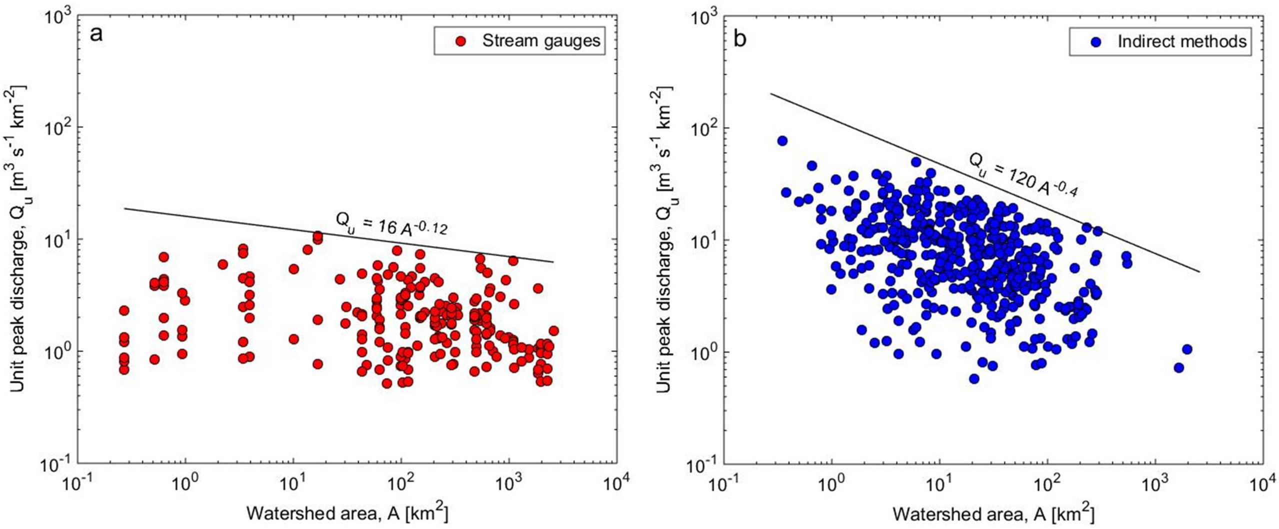
a
Stream gauges
$Q_u = 16\,A^{-0.12}$
Unit peak discharge, Q_u [$m^3\,s^{-1}\,km^{-2}$]
Watershed area, A [km^2]
b
Indirect methods
$Q_u = 120\,A^{-0.4}$
Unit peak discharge, Q_u [$m^3\,s^{-1}\,km^{-2}$]
Watershed area, A [km^2]

Figure 5